# Radiotherapy for Temporal Bone Cancers

29

Sweet Ping Ng and G. Brandon Gunn

## Abbreviations

| | |
|---|---|
| CRT | Chemoradiotherapy |
| CT | Computed tomography |
| FDG | Fluorodeoxyglucose |
| Gy | Gray |
| IMPT | Intensity-modulated proton therapy |
| IMRT | Intensity-modulated radiation (photon) therapy |
| IORT | Intraoperative radiation therapy |
| MRI | Magnetic resonance imaging |
| PET | Positron emission tomography |
| PORT | Postoperative radiotherapy |
| SCC | Squamous cell carcinoma |
| VMAT | Volumetric modulated arc therapy |

## Introduction

Temporal bone cancer is an extremely rare head and neck cancer with relatively poor prognosis in advanced cases. Although squamous cell carcinoma (SCC) is the most common pathology in temporal bone cancer, temporal bone SCC only accounts for 0.2% of all head and neck SCCs [1]. Given its rarity, meaningful comparison of different staging systems and treatment outcomes has proven to be challenging. To date, there has been no universally accepted staging system or consensus of optimal treatment strategies.

Radiotherapy plays a major role in the multimodality management of head and neck cancer patients. There has been retrospective case series in temporal bone cancers suggesting that the addition of postoperative radiotherapy (PORT) to definitive surgery improves outcomes [2–7]. In the postoperative setting, the general indications for adjuvant radiotherapy include positive or close (<5 mm) margins [8], nodal involvement, nodal extracapsular extension, T3 or T4 disease [9, 7], and perineural and lymphovascular invasion [8].

The use of radiotherapy, with or without concurrent chemotherapy, in the definitive setting has been examined recently in patients with locally advanced disease. A recent study by Morita et al. [10] showed a similar 5-year overall survival for patients with T3 and T4 disease treated with definitive chemoradiotherapy (CRT) (52.1%) and those who had surgery followed by adjuvant radiotherapy with/without chemotherapy (55.6%). Shinomiya et al. [11] observed similar clinical outcomes (5-year overall survival 60%; 5-year disease-free survival 60%) in their cohort of 10 patients who had modern staging with CT, MRI, and PET and treated with modern radiotherapy techniques. Takenaka et al. [12] evaluated the use of CRT in a meta-analysis on 752 locally advanced SCCs of the external auditory canal cases in 28 papers published between 2006 and 2013. They reported better 5-year overall survival in the preoperative CRT (85.7%) group compared to surgery ± radiotherapy (53.3%), definitive CRT (43.6%), and adjuvant CRT (0%). Although this meta-analysis showed no patients who had adjuvant CRT alive at 5 years, there were only eight patients included in the analysis. Therefore, the number of adjuvant CRT patients was too small to come to any significant or definitive conclusions with regard to the efficacy of adjuvant CRT in this meta-analysis.

Apart from external beam radiotherapy, brachytherapy has been used as boost treatment in cases where tumors were excised with positive margins or in cases of recurrences after external beam radiotherapy [6]. However, caution will need to be taken with brachytherapy to this area, as there is a moderate to high risk of soft tissue necrosis and osteonecrosis of the temporal bone.

Intraoperative radiotherapy (IORT) was explored by Cristalli et al. [5] as an approach to improve local control in middle ear tumors. In this retrospective study, the team delivered IORT (12 Gy) followed by postoperative radiotherapy

S. P. Ng, M.B.B.S., BMedSci (✉) · G. Brandon Gunn, M.D.
Department of Radiation Oncology, The University of Texas M.D. Anderson Cancer Center, Houston, TX, USA
e-mail: SPNg@mdanderson.org; GBGunn@mdanderson.org



P. W. Gidley, F. DeMonte (eds.), *Temporal Bone Cancer*, https://doi.org/10.1007/978-3-319-74539-8_29

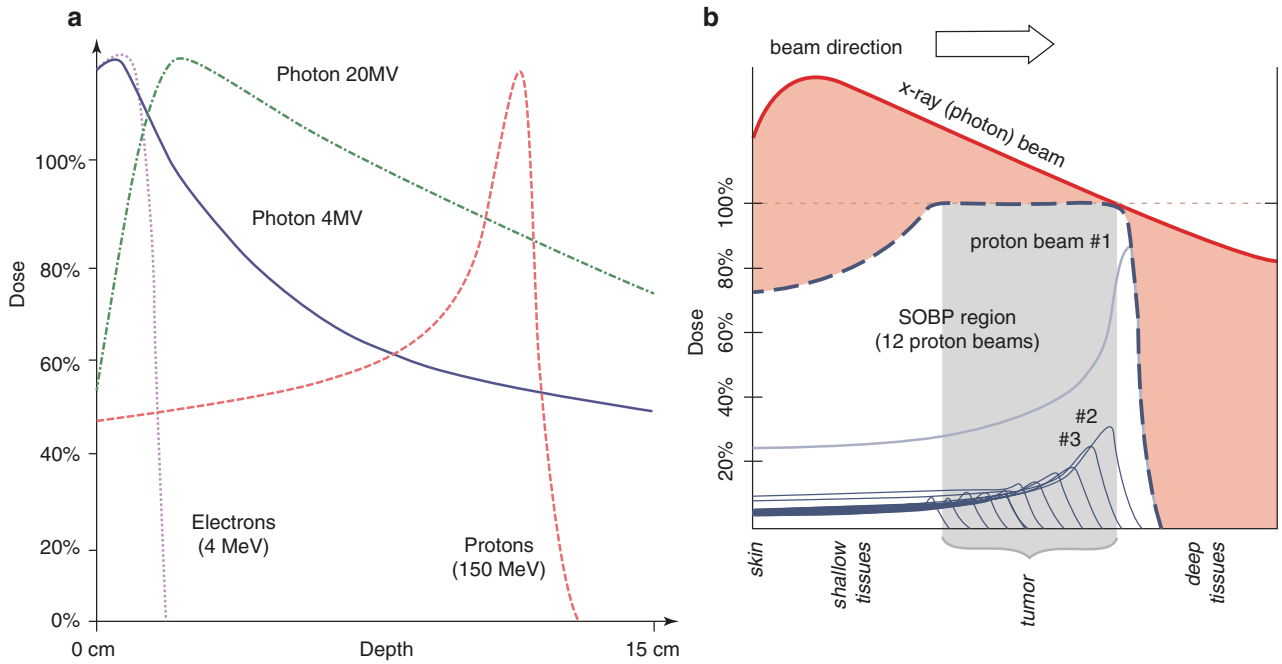


**Fig. 29.1** (**a**) Depth-dose curves for photons (X-rays), electron, and proton beams, highlighting the dose distribution differences between each modality. (**b**) Depth-dose curves for photon and proton beams showing the steep dose drop-off for proton beam after the target area. Image **a** taken from https://en.wikipedia.org/wiki/Proton_therapy#/media/File:Comparison_of_dose_profiles_for_proton_v._x-ray_radiotherapy.png. Image **b** taken from https://commons.wikimedia.org/wiki/File%3ADose_Depth_Curves.svg

to 50 Gy to 13 patients. The 5-year local control, disease-free survival, and overall survival rates were 68%, 61%, and 69%, respectively. Partial necrosis of the flap was observed in three patients, although complete healing was eventually achieved with dressings.

As a general principle, the role of radiotherapy in a postoperative setting is to eliminate microscopic disease and improve locoregional control. Radiation therapy is estimated to decrease the risk of locoregional relapse by 50–60%.

The total radiation doses for a standard postoperative case with clear surgical margins are 60 Gy to postoperative tumor and involved nodal bed, 56–58 Gy to surgical bed and clinical high-risk areas, and ~54 Gy to undissected elective regions (standard clinical risk). At least 56–58 Gy will be delivered to the surgical scar with a safe margin to ensure adequate coverage of the scar. The surgical scar is typically marked with CT radiopaque wire, to improve visibility of the scar location on CT images, and a surface bolus is fabricated at simulation and used during treatment to ensure adequate surface dose when photon-based therapy is used.

There are several different radiation modalities including photons, electrons, and protons and various radiation techniques that can be utilized. The decision of which modality to use for each patient is considered on a case-by-case basis, depending on site of treatment, depth of target, field size, and surrounding normal tissues that require sparing. Generally, electrons are used for superficial targets, while photons and protons are utilized when the target also includes deeper tissues. Figure 29.1 summarizes the physical properties of each modality.

## Case Studies

Here, we present several cases to highlight the different radiation modalities and techniques that can be utilized in patients with temporal bone tumors to increase the efficacy to radiation treatment delivery and reduce toxicities of treatment.

### Case 1

This case showcases the use of intensity-modulated proton therapy (IMPT) treatment technique to deliver postoperative radiation to the skull base area while sparing nearby critical neural structures such as the brain stem, spinal cord, and contralateral hearing apparatus. IMPT is a highly precise technique utilizing pencil beam scanning to deliver proton treatment in a highly conformal fashion.

A 58-year-old female of good performance status presented with a history of chronic bilateral hearing loss, left ear

pain, intermittent vertigo, and otorrhea, on a background of multiple tympanostomy tubes in her left ear over several years, and more recently a tympanomastoidectomy and multiple revision surgeries for an adenoma in her left middle ear. Biopsy of tumor within the left Eustachian tube from her most recent revision surgery revealed moderately differentiated intestinal-type adenocarcinoma.

Clinical examination revealed a normal left outer ear with a well-healed postauricular scar consistent with previous surgery. The left ear canal was filled with tenacious secretion, and there was a polypoid tumor within the posterior mesotympanum. There was left hypoacusis. Other cranial nerve examination was unremarkable. Nasopharyngoscopy examination revealed a tumor nodule within the left Eustachian tube.

Staging imaging including CT, MRI, and PET showed an extensive intratympanic and intramastoid tumor within the left temporal bone (Figs. 29.2, 29.3, and 29.4). The tumor was heterogeneously hypointense on T1 and hyperintense on T2 reminiscent of fluid or soft components. The left occipital bone was involved, extending posteriorly from the mastoid. There was no evidence of distant metastatic disease on PET.

Given the extent and recurrent nature of disease, she was recommended for definitive surgery followed by postoperative radiation therapy at the multidisciplinary tumor board conference.

At surgery, a lateral temporal bone resection with removal of the ear canal, excision of extratemporal soft tissue mass, resection of extradural middle and posterior fossa skull base tumor, superficial parotidectomy, and selective left neck dissection and reconstruction were performed. Operative findings described an extensive tumor with involvement into the extratemporal soft tissues of the skull base and extension along the retrosigmoid dura extratemporally. Disease involved all aspects of the temporal bone, including the middle ear, mastoid, retrofacial air cells, and along the jugular bulb into the petrous apex and Eustachian tube. Tumor was seen to extend from the mastoid into the upper sternocleidomastoid muscle.

Final histopathology confirmed intestinal-type adenocarcinoma involving skeletal muscle, soft tissue, and bone, with no evidence of lymphovascular or perineural invasion. The tumor involved the muscle and cartilage from the Eustachian tube, the retrosigmoid tissue, the stylomastoid foramen, tissue medial to the carotid, tissue from middle ear, retrofacial air cells, and the mastoid cavity. One node within the left parotid was positive for tumor. There was no tumor identified in left neck dissection levels 2A to 3. The condyle of the mandible was not involved, and resection margins were clear. Figure 29.5 showed the postoperative changes evident on CT obtained after surgery.

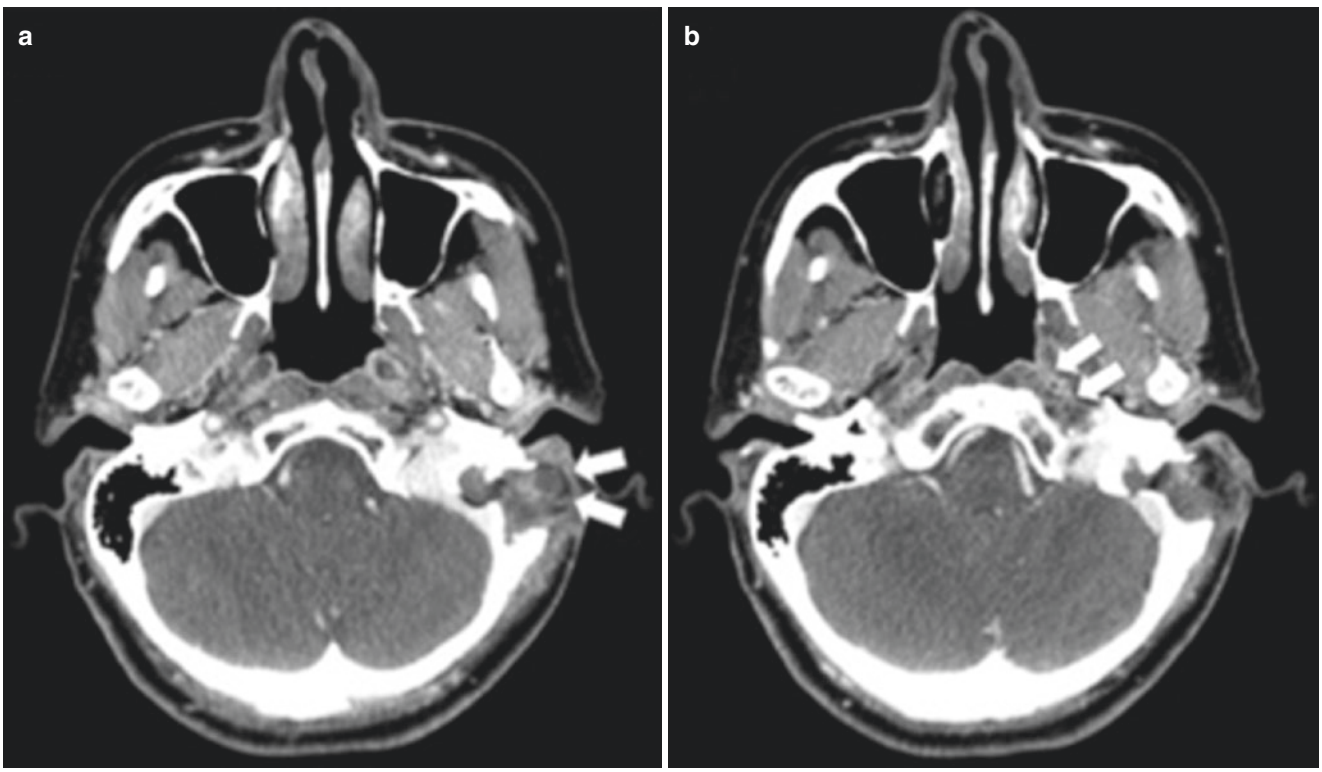


**Fig. 29.2** CT of patient 1 depicting (**a**). The large mastoidectomy defect filled with tumor that enhances mildly with tumor behind the left stylomastoid foramen (arrows) and (**b**) subtly enhancing tumor in the left Eustachian tube

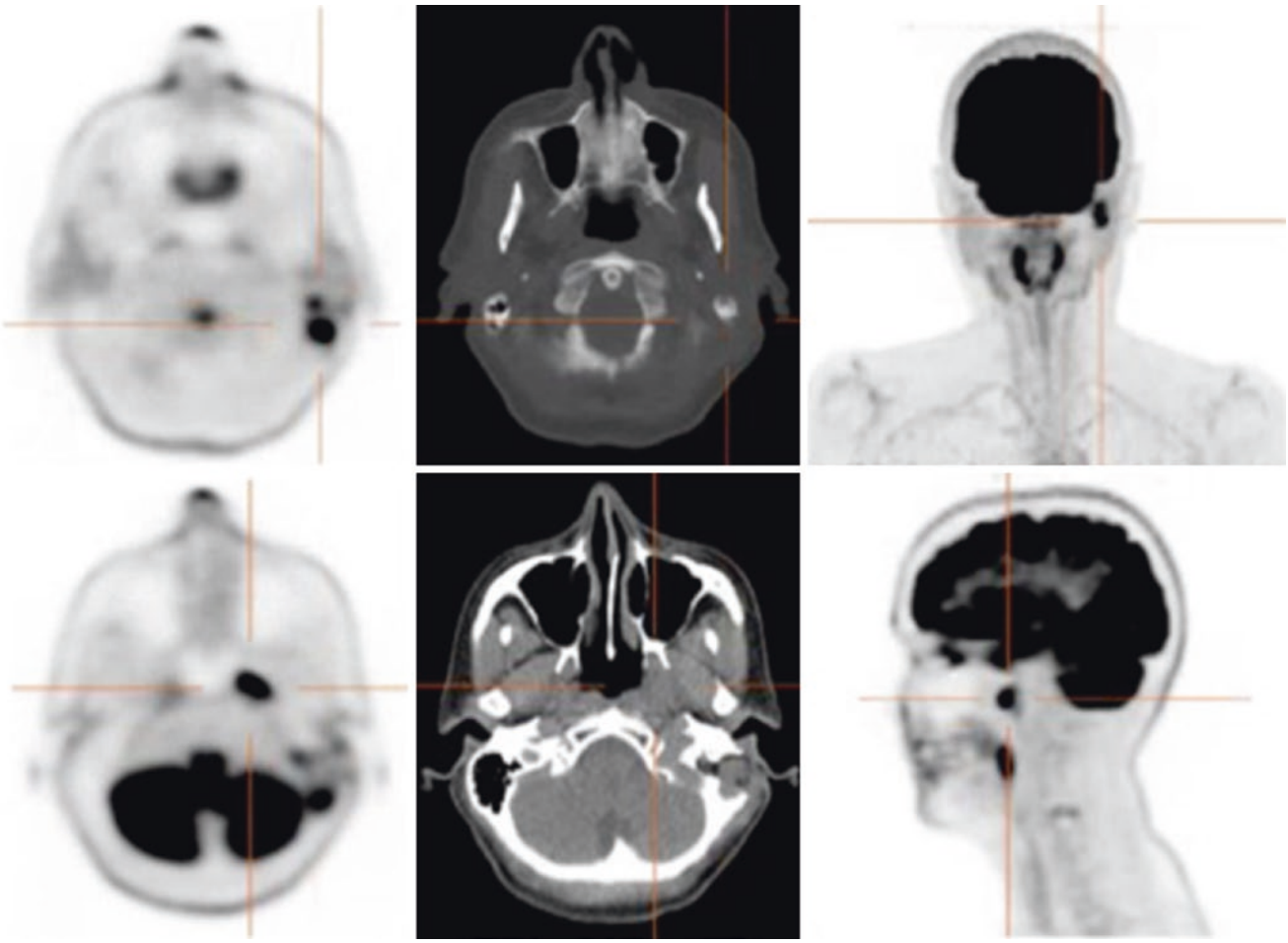

**Fig. 29.3** PET showing the FDG-avid lesion correlating with the abnormality on CT within the left temporal region and left Eustachian tube

Approximately a fortnight following surgery, she was simulated for radiation therapy delivered using IMPT technique to facilitate maximal sparing of her critical structures, in particular the temporal lobe, brain stem, spinal cord, and contralateral cochlea especially when she had complete hearing loss on the affected side. The advantage of proton therapy is the rapid dose falloff after target volume; and hence, in this case, this technique maximizes sparing of her critical neural structures while delivering minute to no dose to her contralateral cochlea.

The patient was brought to the proton therapy simulation suite. A bite block was integrated, and a customized thermoplastic mask was fabricated and secured over the patient. Provisional isocenter was placed and CT images were obtained. The images were transferred to the treatment planning system for contouring and treatment planning purposes. Target volume encompassed the postoperative bed with planned 66 Gy to the high-risk areas (tumor bed) and 58 Gy to the unaffected operative bed (dissected neck) (Fig. 29.6). She was treated to a total dose of 66 Gy in 33 daily fractions over 6.5 weeks.

The patient tolerated the treatment well with grade 2 skin reaction and grade 1 oral mucositis at the end of treatment. Follow-up clinical examination and MRI at 3 years did not reveal any signs of locoregional recurrence or significant late toxicity of treatment.

## Case 2

This case poses a diagnostic conundrum given the initial difficulty in detecting perineural invasion radiologically to account for the patient's symptoms. In this case, intensity-modulated radiation therapy (IMRT) technique was used. IMRT utilizes photon beams and delivers highly conformal radiation doses to the target volume via multiple beams while limiting dose to the surrounding normal tissues.

A 67-year-old male, of good performance status, with a long history of sun exposure and multiple treated non-melanomatous cutaneous carcinomas, presented with a 5-year history of gradual worsening left facial paresthesia and subsequently left facial paralysis. His past medical history revealed

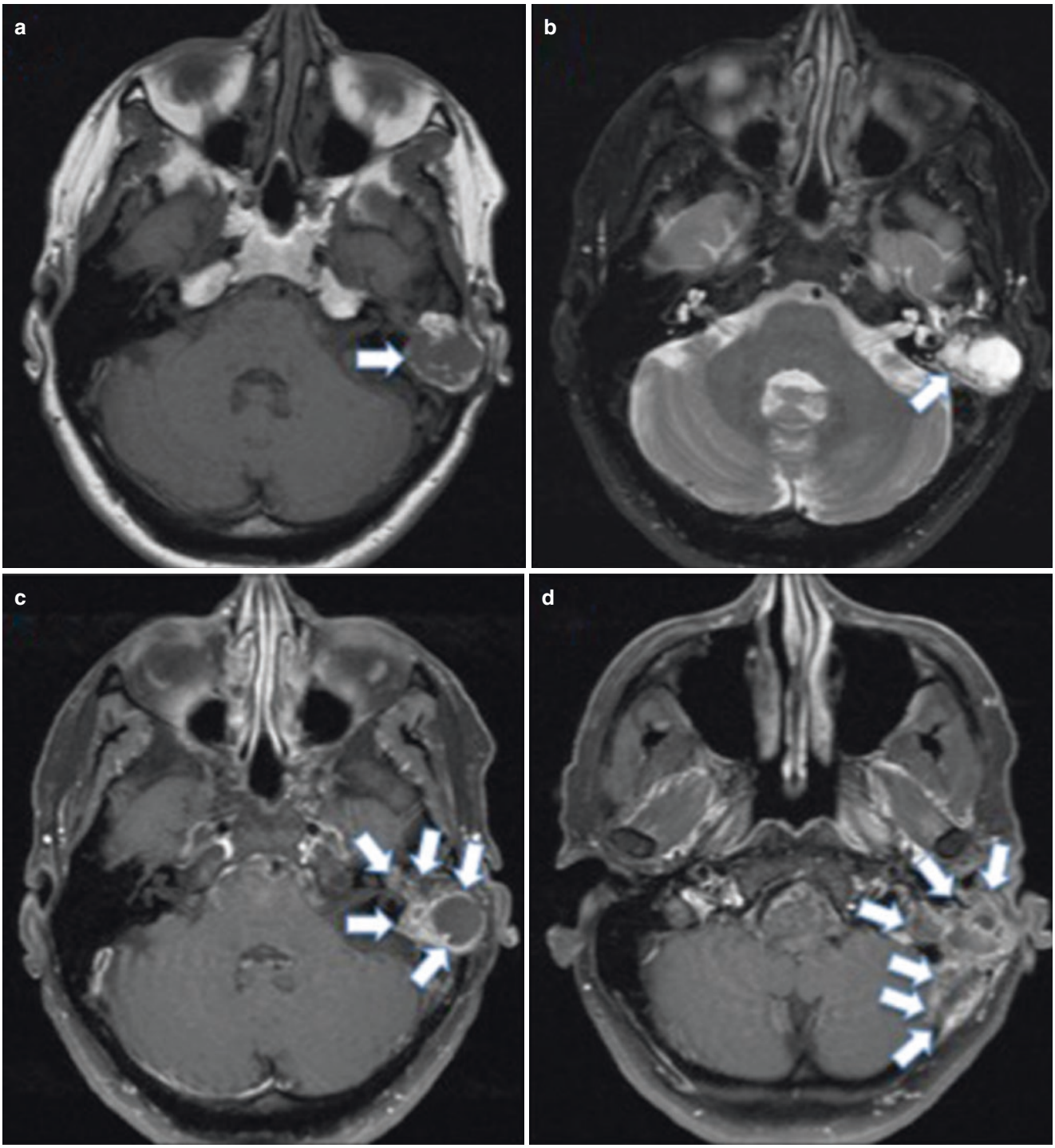


**Fig. 29.4** MRI showing the extent of tumor recurrence. The tumor was heterogeneously hypointense on T1 (**a**) and hyperintense on T2 (**b**), with peripheral ring-type enhancement (**c**). Image **d** and **e** showed involvement of the left occipital bone extending posteriorly from the mastoid. The extent of disease is shown in a representative coronal section (**f**)

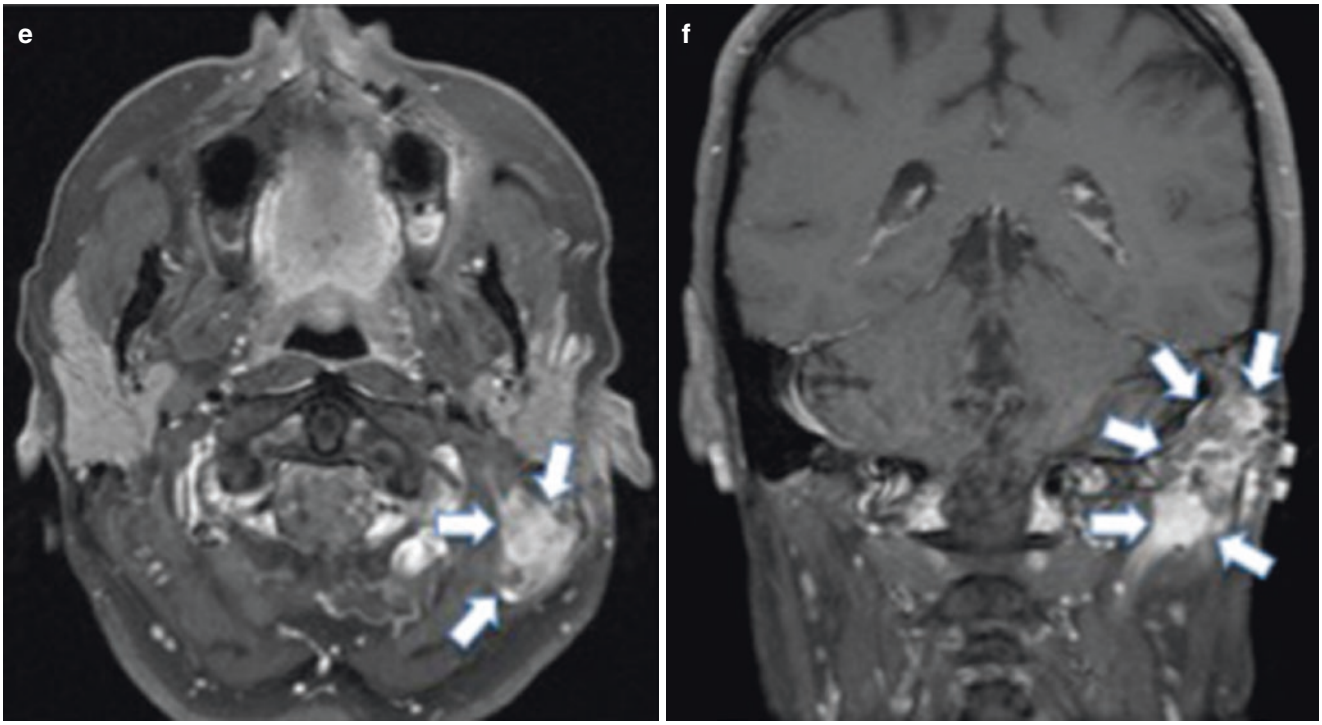


**Fig. 29.4** (continued)

**Fig. 29.5** CT after surgical resection and flap reconstruction

a previous left cheek basal cell carcinoma that was excised via Mohs surgery 10 years prior. Numerous imaging evaluations including MRIs over several years were unrevealing of a specific cause for his facial paralysis and facial paresthesia.

Physical examination revealed a complete left facial paralysis and a palpable subcutaneous nodule near the surgical scar in his left cheek. Facial sensation was intact. There was no palpable cervical lymphadenopathy.

Repeat MRI subsequently showed abnormal enhancement of the left facial nerve, posterior genu and the descending segment into the stylomastoid foramen, and the proximal extracranial main facial trunk (Fig. 29.7). There was a speculated subcutaneous mass measuring 1.6 cm within the area of previous Mohs surgery, concerning of subcutaneous skin cancer.

A fine needle aspiration and a core biopsy of the left cheek nodule yielded no malignant cells. Following discussion at the multidisciplinary tumor board conference, the patient was dispositioned to surgery followed by postoperative radiotherapy given the extent of facial nerve involvement.

The patient underwent excision of left subcutaneous nodule, total parotidectomy, selective neck dissection levels II–III, complete mastoidectomy, and resection of the left facial nerve. This was followed by reconstruction of the left cheek defect with free anterolateral thigh flap, an 11 cm nerve graft anastomosed from proximal stump of facial nerve to the marginal branch. A static sling of the left face was performed to correct the left facial palsy defect.

Histopathology confirmed poorly differentiated squamous cell carcinoma with perineural carcinomatous nests within the parotid and perineural involvement of the facial nerve including at the mastoid segment. No lymph nodes were involved.

A month following surgery, the patient was brought to the CT simulation suite. He was positioned on the simulator

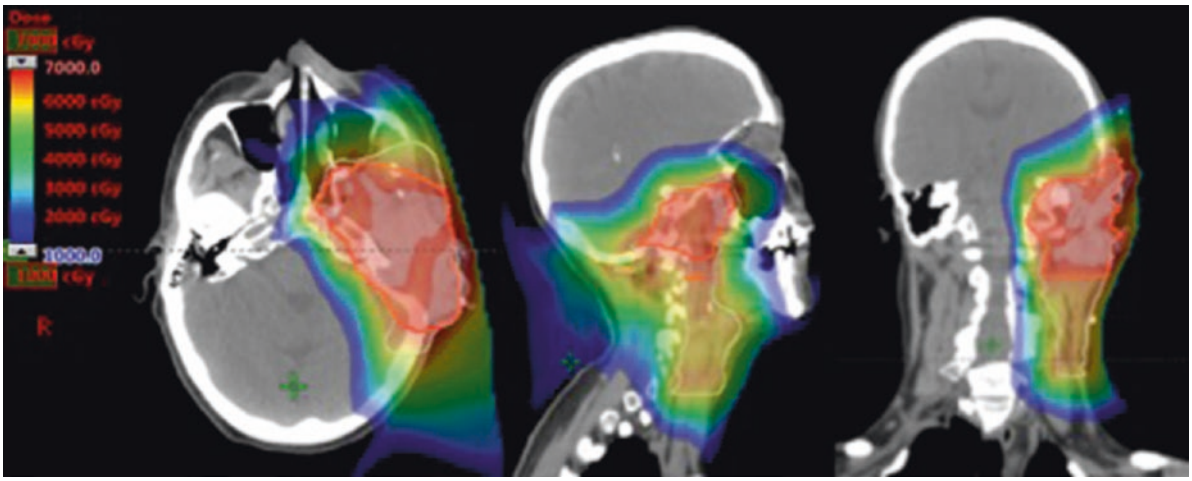


**Fig. 29.6** Representative axial, sagittal, and coronal images of radiation dose distribution plan using IMPT planning, highlighting the rapid dose falloff after target volume contoured (red line,66 Gy; yellow line, 58 Gy)

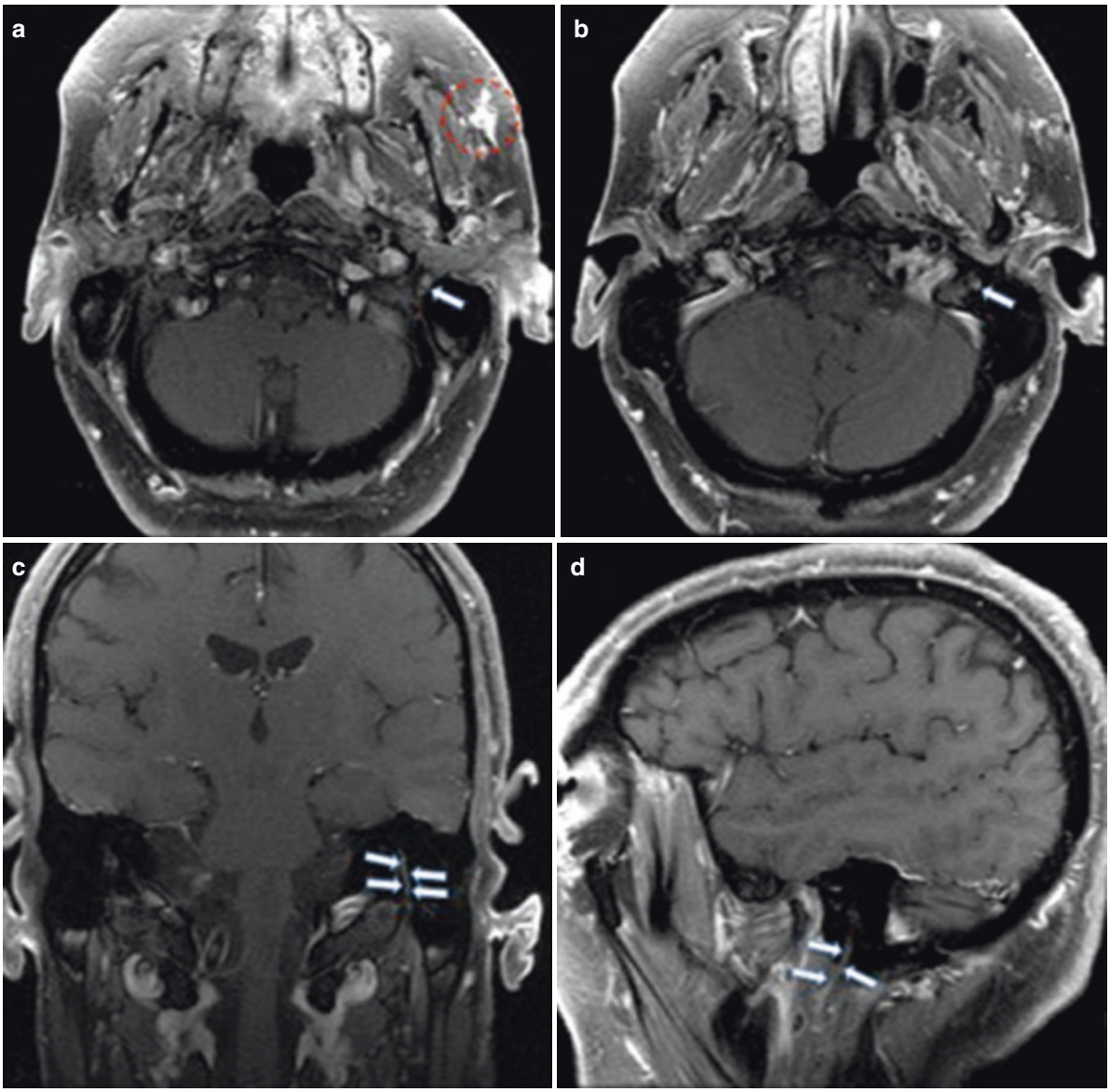


**Fig. 29.7** T1 with contrast MRI images illustrating the subcutaneous mass (dotted red line in image **a**) and the enhancement of the left facial nerve (arrows)

table in the supine position on a headrest. As for most postoperative cases, the surgical scar and flap reconstruction was wired with CT radiopaque marker to assist with target volume delineation. A custom tongue-deviating stent was placed into the oral cavity. A 5 mm custom bolus was fabricated with a 1–1.5 cm margin to the surgical scar. The bolus is made of soft tissue-equivalent material and is used to ensure sufficient surface dose. A tissue-equivalent material was placed into the left ear and taped the ear flat to the neck to reduce contour irregularities and tissue inhomogeneity during radiation treatment planning and delivery. A 2 mm custom bolus was placed over the neck dissection scar. A customized thermoplastic mask was used for immobilization (Fig. 29.8). Non-contrast CT images were taken from the top of the head to the carina. These images were transferred to the treatment planning software system for contouring and CT-based treatment planning.

The patient was treated using IMRT technique. A total dose of 60 Gy was delivered to the tumor bed with a boost to facial canal and to the soft tissue under the flap to 66 Gy. Areas at intermediate risk (dissected uninvolved areas) received 57 Gy, and low-risk (uninvolved undissected unilateral neck) regions received a dose of 54 Gy. The target volume encompassed the postoperative tumor bed and the facial nerve tracking all the way to its site of origin at the brain stem (Fig. 29.9). Radiation therapy was delivered under daily kV imaging guidance and with concurrent cisplatin (40 mg/m$^2$ weekly).

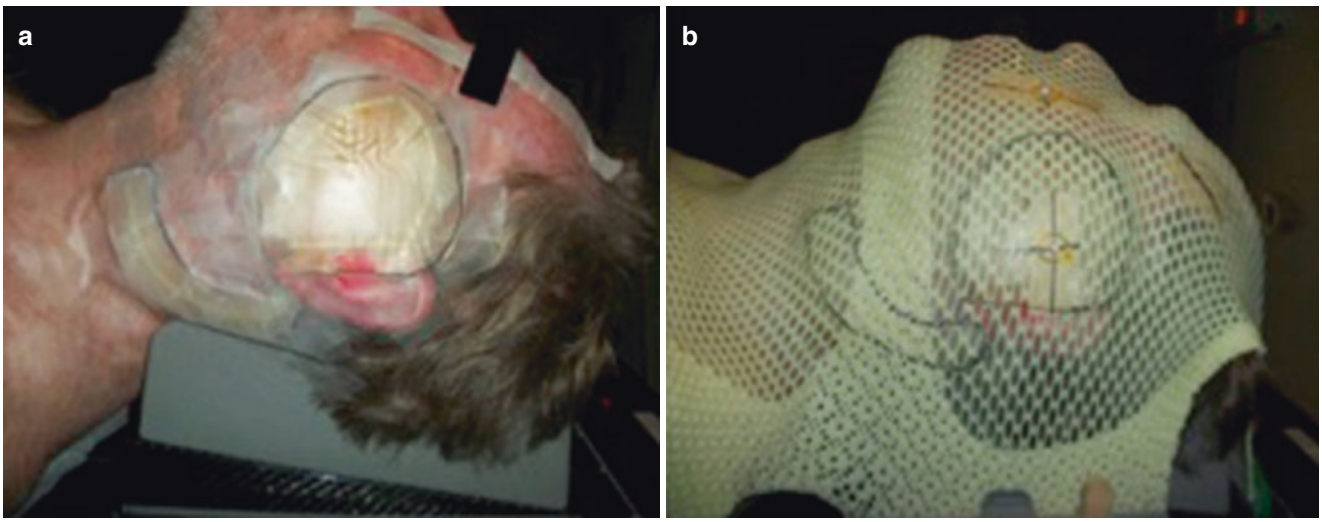


**Fig. 29.8** Simulation. Surgical scars were wired and a custom bolus placed over the scar with a margin to improve dose delivery to skin surface. Tissue-equivalent material (pink) was placed into left ear to reduce tissue inhomogeneity. Finally a thermoplastic mask was placed over patient for immobilization

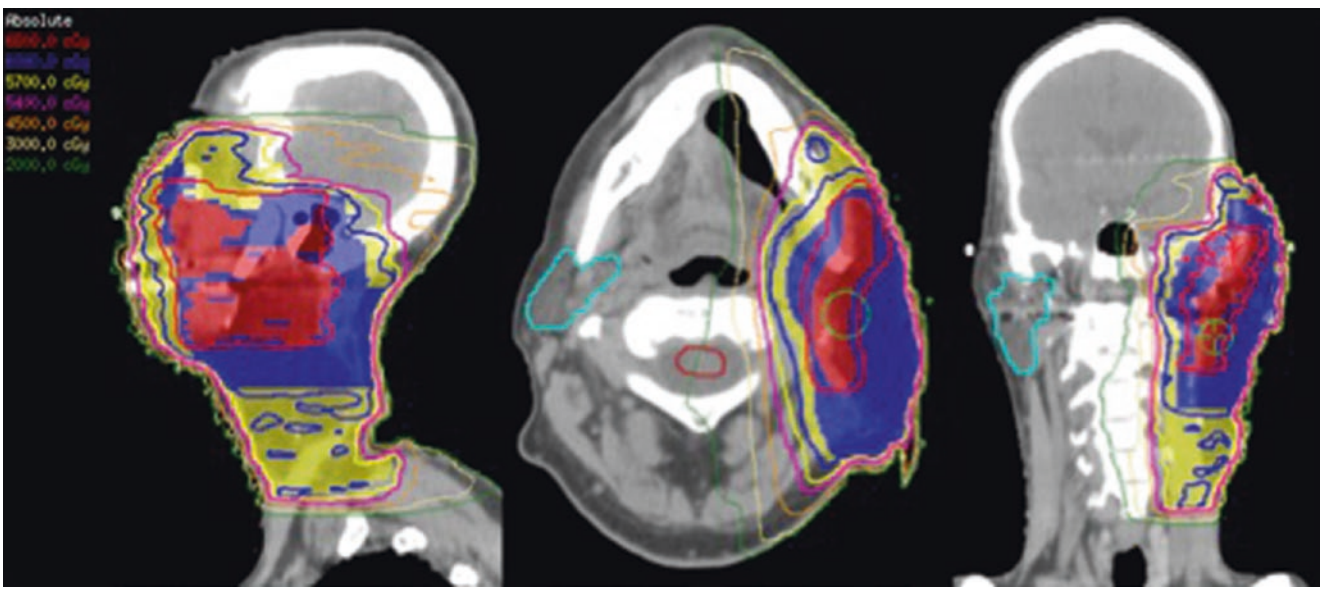


**Fig. 29.9** Final dose distribution plan utilizing IMRT. Note sparing of contralateral parotid gland. Shaded areas indicate contoured target volumes, and lines indicate isodose lines (red, 66 Gy; blue, 60 Gy; yellow, 57 Gy)

He tolerated the treatment well with grade 3 skin reaction and grade 1 oral mucositis at the end of treatment. At 5-year follow-up, he remained disease-free, with no significant late toxicities of treatment.

## Case 3

This case demonstrates the use of IMRT in the definitive setting for a locally advanced non-operable case. Unfortunately, the patient in case 3 subsequently relapsed within the low to no dose region after completion of radiotherapy.

An 81-year-old male, of average performance status (ECOG 2), with a long history of treated non-melanomatous cutaneous carcinomas of the head and neck region, presented with a 1-year history of left-sided facial paralysis. He had a history of biopsy-proven and recurrent left temple squamous cell carcinoma, for which he had superficial therapies and local excision to that region.

Physical examination revealed a complete left facial paralysis with left upper, mid, and lower face asthenia. There was no palpable parotid or cervical lymphadenopathy. There was a surgical scar and lesion within the left temporal scalp.

Biopsy of a left temporal scalp lesion showed moderately differentiated squamous carcinoma invading deep dermis, with no perineural invasion. CT imaging showed postsurgical changes within the left temporal scalp with nodular enhancement along the posterior margin of the left preauricular region (Fig. 29.10).

MRI (Fig. 29.11) showed an extensive lesion extending from the left temporal skin surface to the periosteum of the skull with extensive perineural enhancement and to the vertical portion of the facial nerve within the stylomastoid foramen as well as bright enhancement along the anterior genu of the facial nerve and of the greater superficial petrosal nerve. Additionally, there was abnormal enhancement in left Meckel's cave and along the branches of left cranial nerve V with involvement of V3 and the vidian canal. The left pterygoid muscles and the soft tissues surrounding the glenoid fossa and the temporomandibular joint had abnormal soft tissue involvement or inflammation. Diffuse edema and inflammation around the coronoid process and the fibers of the temporalis muscle were also seen. There was no radiological or clinical evidence of regional nodal or distant metastatic disease.

Given the extensive skull base perineural involvement, the patient was deemed not a surgical candidate and was dispositioned to radiotherapy following discussion at the multidisciplinary tumor board conference with the aim of achieving local control, as progression of perineural disease will undoubtedly be a detriment to his quality of life.

The patient was brought to the CT simulation suite. The nodule along the left temple was palpated, and a CT radiopaque marker was used to wire-out this area with a generous margin of 2–3 cm. The area along this region was covered with a custom 5 mm bolus to ensure adequate surface dose to this region. Similarly, a 3 mm bolus was used in the preauricular region to ensure adequate dose in that region given

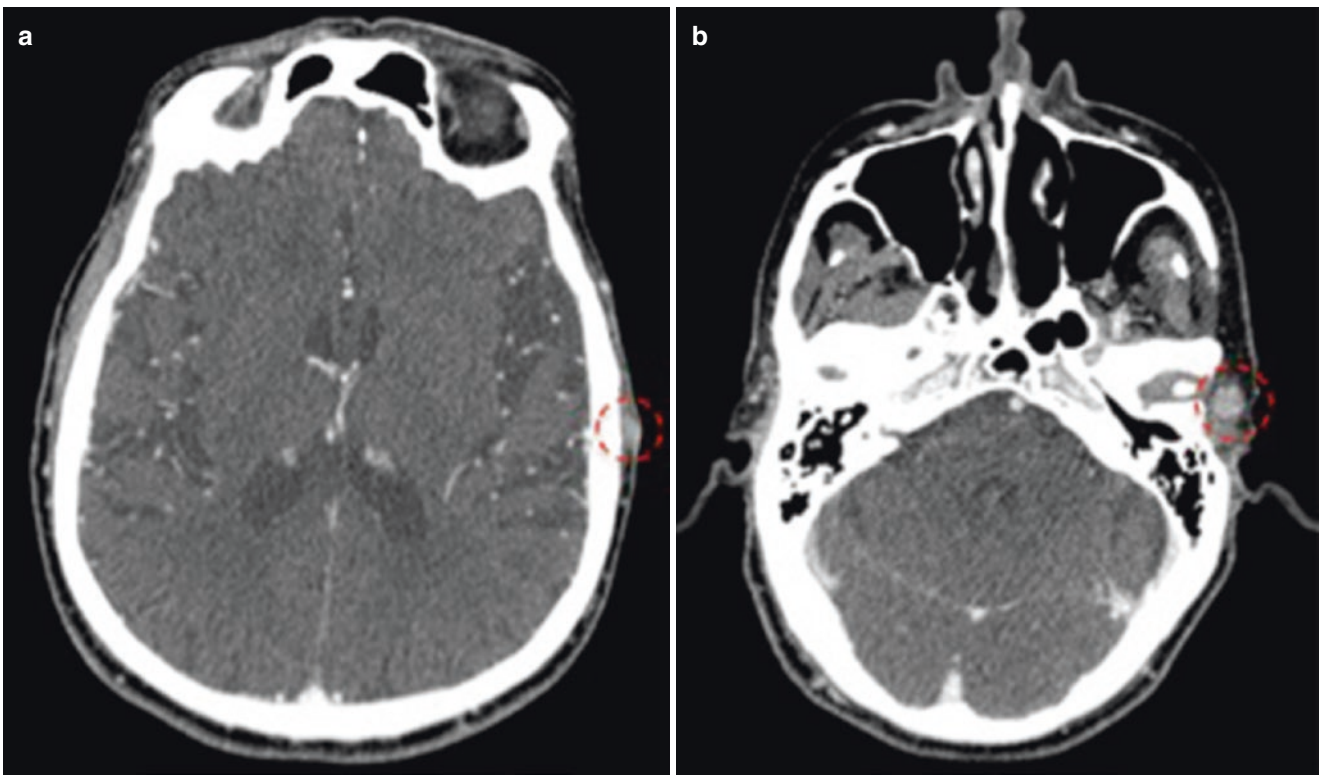


**Fig. 29.10** CT images showing left temporal scalp and preauricular lesion (red dashed circle)

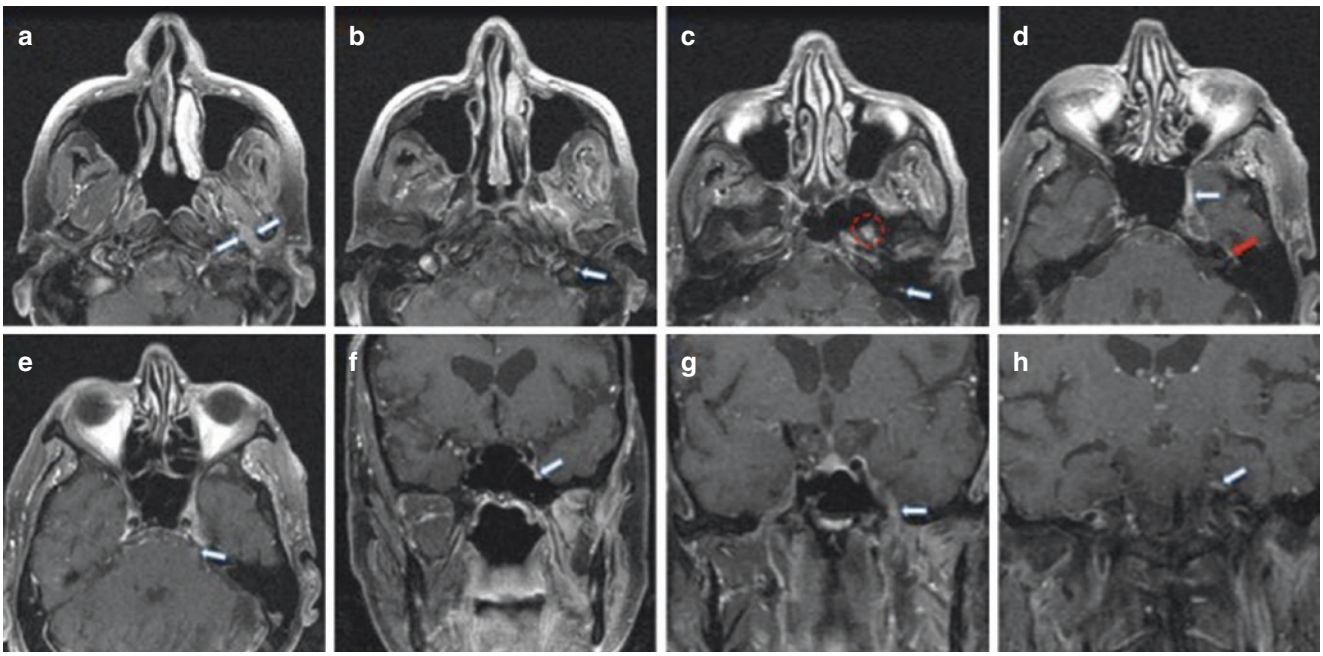


**Fig. 29.11** Pertinent findings on MRI: (**a**) soft tissue involvement surrounding temporomandibular joint. (**b**) Enhancement of facial nerve within the stylomastoid foramen. (**c**) Facial nerve enhancement (arrow) and involvement of temporalis tendon on the coronoid process (red dashed line). (**d**) Enhancement along anterior genu of the facial nerve (white arrow) and the greater petrosal nerve (red arrow). (**f**) Vidian canal involvement. (**g**) Involvement of the V3 nerve through foramen ovale. (**h**) Thickening of the dural folds of Meckel's cave

**Fig. 29.12** Simulation. Surgical scar wired and bolus placed. Tissue-equivalent material placed in his ear. Thermoplastic mask used for immobilization

concern for perineural spread along the facial nerve. His ear was taped back, and tissue-equivalent material was placed within the ear to reduce patient surface contour irregularities (Fig. 29.12). An intraoral stent was placed, and a customized thermoplastic mask was created to immobilize his head, neck, and shoulders in the intended treatment position. Non-contrast CT images were obtained for treatment planning purposes.

The patient was treated using intensity modulation therapy to a total dose of 69.96 Gy in 33 fractions with concurrent erlotinib on a clinical trial. Intermediate- and lower-risk sites were also treated simultaneously to lower doses. The target volume encompassed the left temple region as well as the sites of involvement along cranial nerves V and VII tracking all the way to their origin at the brain stem (Fig. 29.13). Treatment was delivered under daily kV imaging guidance allowing daily bony alignment to reproduce position at simulation and ensure treatment delivery accuracy.

The patient tolerated the treatment well with grade 3 skin reaction and grade 1 oral mucositis at the end of treatment. The patient remained disease-free for 18 months posttreatment. He subsequently developed symptomatic left-sided neck swelling and neuropathic pain. Imaging was concerning for perineural tumor spread along the left greater auricular nerve to C2 (Fig. 29.14). The patient passed away 3 months after.

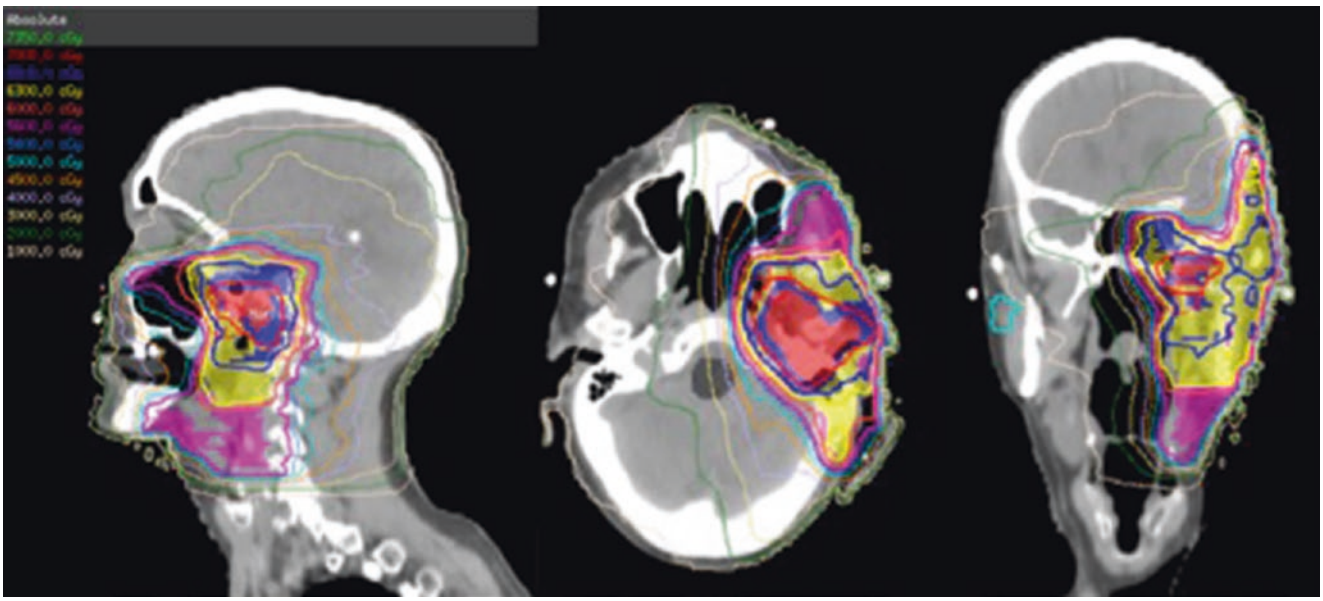

**Fig. 29.13** Representative images of dose distribution. Shaded area: red, 69.96 Gy; blue, 66 Gy; yellow 63 Gy; pink, 55 Gy

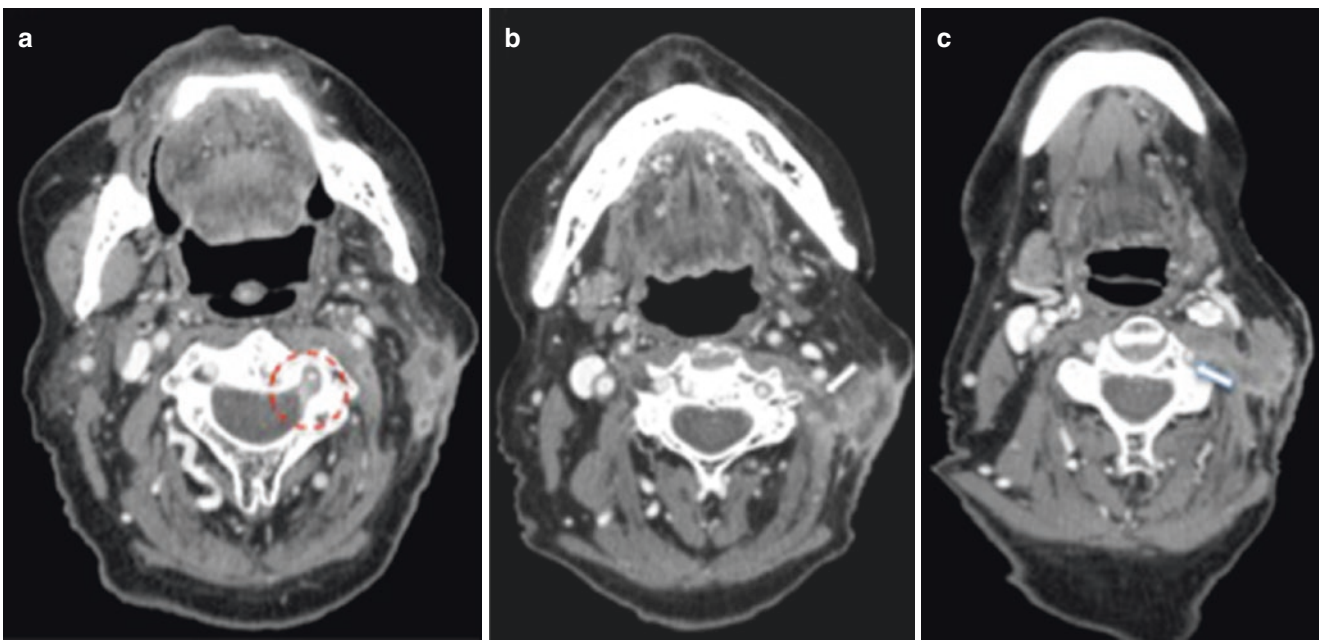


**Fig. 29.14** Recurrence seen on CT imaging. (**a**) Epidural extension via neural foramen at C2. (**b**) Involvement of C2 spinal nerve and mass behind sternocleidomastoid muscle. (**c**) Tumor surrounding left vertebral artery at level of vertebral foramen

## Case 4

This case demonstrates the use of IMRT in the definitive setting for a locally advanced non-operable case. This patient had no evidence of disease at 5-year follow-up after treatment. Cases 3 and 4 highlight that a high dose of radiation is effective in providing local control and the extent of treatment fields/volumes needs considerable thought during treatment planning to achieve a balance between larger treatment fields (i.e., probable better local control) and increased treatment toxicity.

An 88-year-old male, of good performance status (ECOG 1), with significant cardiovascular disease history, presented with recurrent basal cell carcinoma of his right ear for which he had at least seven surgeries over the past 30 years. He was found to have a right preauricular lesion which was excised with positive radial and deep margins. Histology once again confirmed infiltrating basal cell carcinoma.

Physical examination revealed a shortened and narrowed right external auditory meatus consistent with surgical changes. The bony ear canal and tympanic membrane appeared normal. The left external ear, meatus, and tympanic membrane were normal. There was no gross cranial neuropathy or palpable cervical lymphadenopathy. CT imaging showed the soft tissue recurrence abutting the mandibular condyle and temporomandibular joints without obvious bony involvement (Fig. 29.15). Formal audiology assessment revealed moderate to severe bone conduction hearing loss in the right ear.

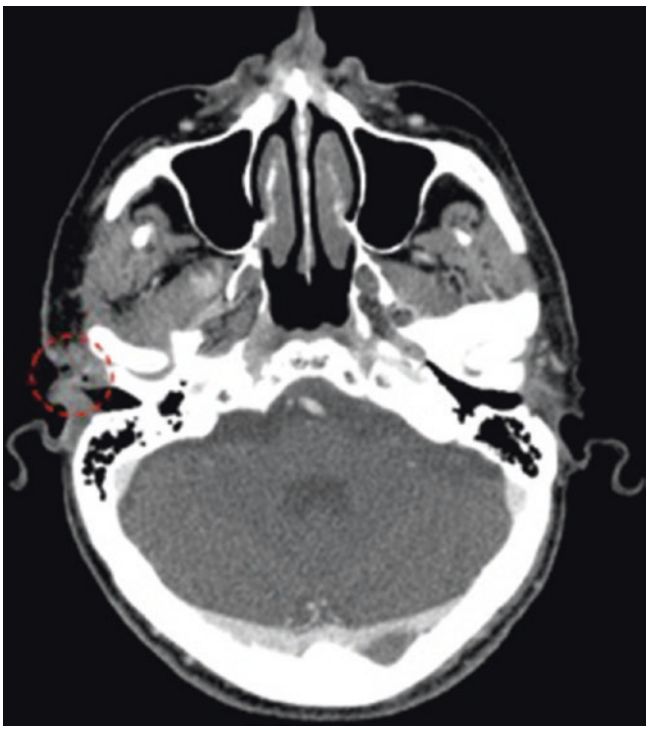

**Fig. 29.15** Representative CT image showing right preauricular lesion (red dashed circle)

He was deemed not a suitable surgical candidate due to his extensive cardiovascular history and was dispositioned to definitive radiotherapy following discussion at the multidisciplinary tumor board conference.

The patient was brought to the CT simulation suite. His ear was taped back, and tissue-equivalent material was placed within the ear to reduce any contour irregularities (Fig. 29.16). A customized thermoplastic mask was created to immobilize his head in the intended treatment position. Non-contrast CT images were obtained for treatment planning purposes.

He was treated using IMRT technique to a total dose of 66 Gy in 30 fractions to the gross tumor, with 60 Gy to surgical bed and 57 Gy to adjacent at-risk soft tissues (Fig. 29.17).

He tolerated radiotherapy very well with grade 3 skin reaction within the posterior aspect of the auricle. His 3-year follow-up imaging (Fig. 29.18) and his 5-year clinical follow-up showed no evidence of tumor recurrence. Audiology assessment at 3 years after radiotherapy revealed no significant change in his hearing function compared to pre-radiotherapy levels.

## Case 5

This case highlights the fact that each radiotherapy plan is considered on a case-by-case basis, tailoring treatment target volumes to an educated estimate of each patient's risk of locoregional relapse. This patient had a localized low-grade ear canal tumor whereby postoperative radiotherapy was delivered to the tumor and surgical beds only, as her risk of regional nodal relapse is estimated to be low, thereby reducing the volume of tissue treated and risk of acute and long-term complication of radiotherapy.

A 62-year-old lady of good performance status presented with several months history of left ear fullness and drainage. Clinical examination revealed a left ear canal mass.

She proceeded to have a left temporal bone excision, left parotidectomy, and left facial nerve biopsy. Final histopathology confirmed low-grade squamous cell carcinoma within the temporal bone involving the external auditory canal. The tumor was excised with clear margins, with no evidence of perineural or lymphovascular invasion. Given the bony involvement of tumor, postoperative radiotherapy was recommended.

She was brought to the CT simulation suite. The surgical scar was wired-out with a CT radiopaque marker, and a tissue-equivalent material was placed in the left ear canal. A customized thermoplastic mask was created to immobilize her head, neck, and shoulders in the intended treatment position (Fig. 29.19). Non-contrast CT images were obtained for treatment planning purposes.

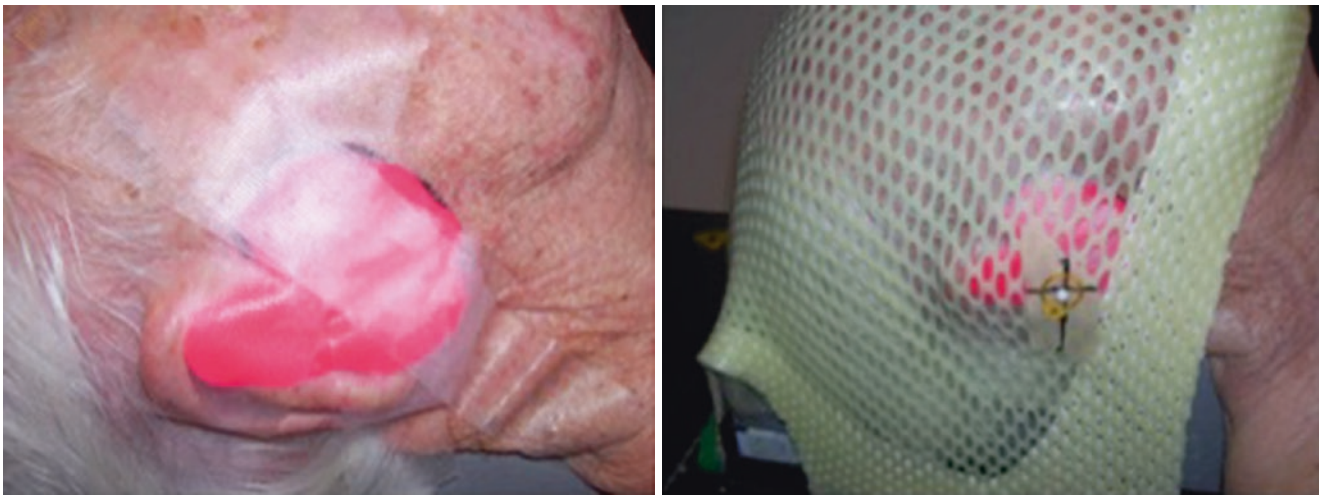

**Fig. 29.16** Simulation. Tissue-equivalent material placed in his ear. Thermoplastic mask used for immobilization

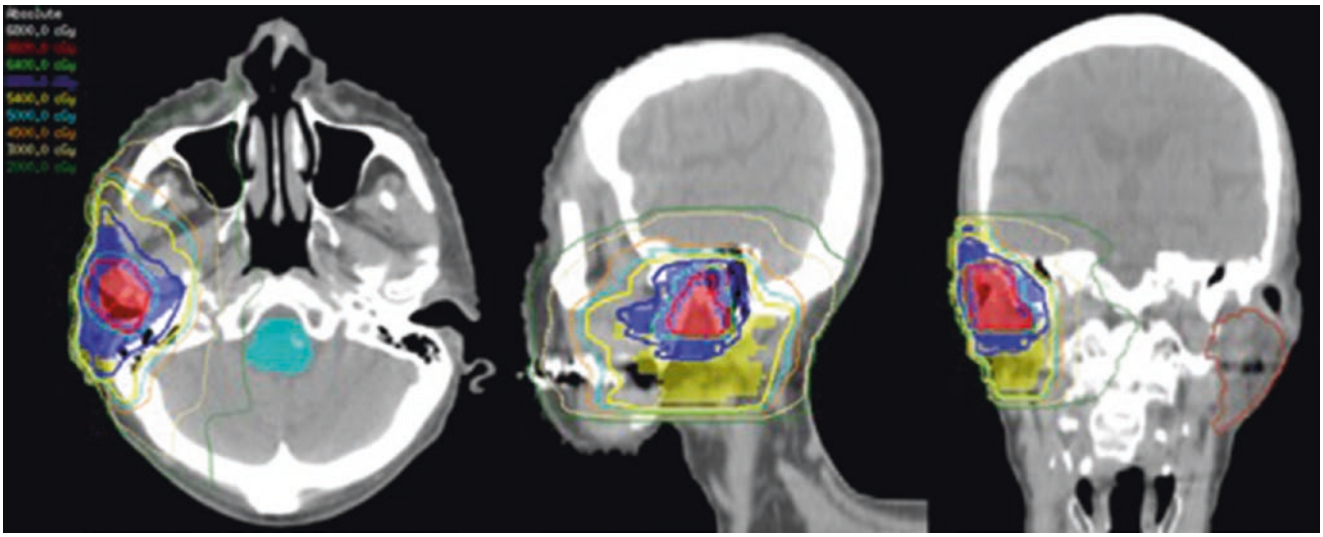

**Fig. 29.17** Representative images of dose distribution. Shaded area: red, 66 Gy; blue, 60 Gy; yellow, 56 Gy

The patient was treated using volumetric arc therapy (VMAT) to a total dose of 60 Gy in 30 fractions. VMAT technique, a way of delivering photon radiation in an arc fashion, was chosen in this case to improve dose homogeneity delivered to the target volume while limiting dose to the contralateral normal tissues. The non-involved surgical bed was treated to a lower dose of 56 Gy. The target volume encompassed the tumor bed and non-involved surgical bed (Fig. 29.20). The draining nodal groups were not electively covered since her risk of nodal metastases was estimated as low (<15%), her tumor was low grade with no adverse features, and her tumor was excised with clear margins. Treatment was delivered under daily kV imaging guidance.

The patient tolerated the treatment very well with skin erythema and mild desquamation at the end of treatment. She recovered well from the acute effects of radiotherapy. She has ongoing follow-up with her surgical team.

## Acute Effects of Radiotherapy During Treatment

In general, apart from fatigue, the acute effects of radiotherapy are local and limited to the radiotherapy treatment fields. Therefore, the side effect profile of radiotherapy can vary from patient to patient, depending on the patient's general status (comorbidities, performance status, medications, nutritional status), surgical site and healing, radiological and pathological findings, and radiotherapy treatment factors (total dose, dose/fraction, fields, treatment modality).

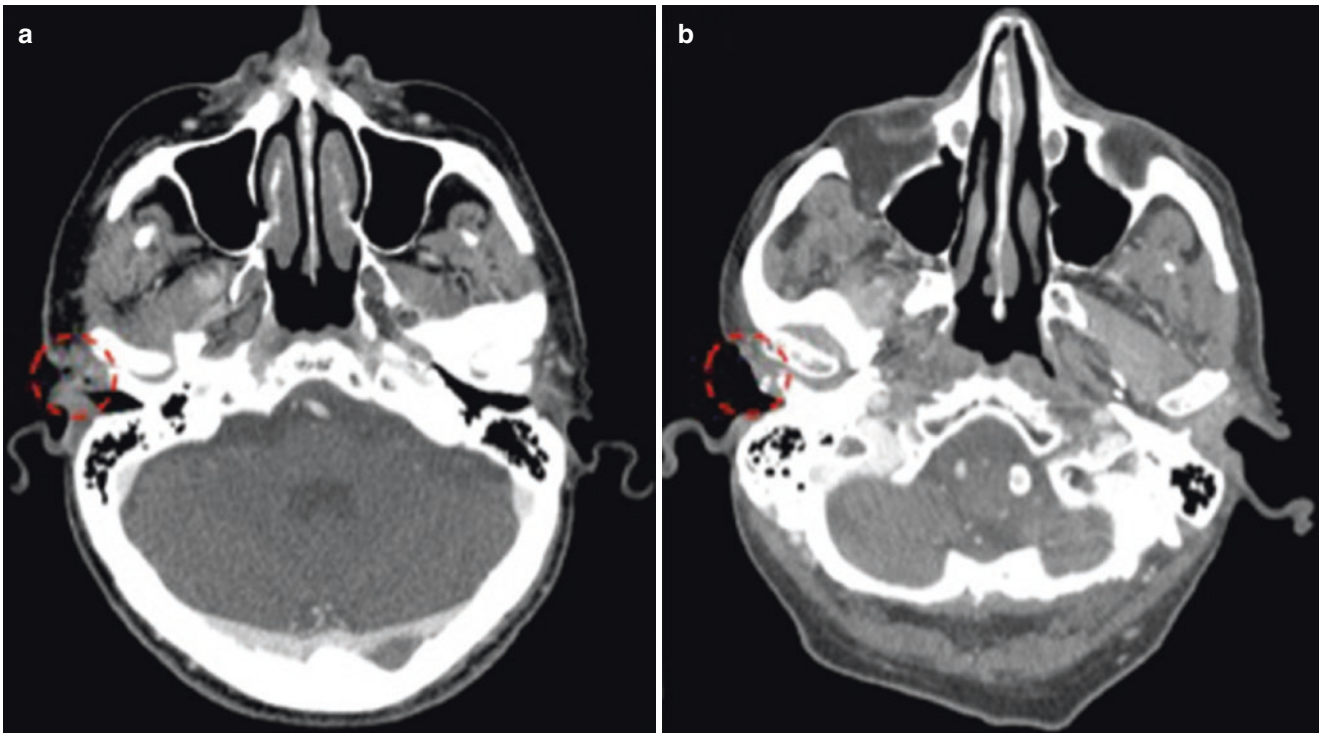


**Fig. 29.18** Comparison of images before (**a**) and 3 years after (**b**) radiotherapy, highlighting the absence of tumor

**Fig. 29.19** Simulation. Postauricular surgical scar wired and tissue-equivalent material place within the left ear canal to reduce tissue inhomogeneity. Thermoplastic mask used for immobilization

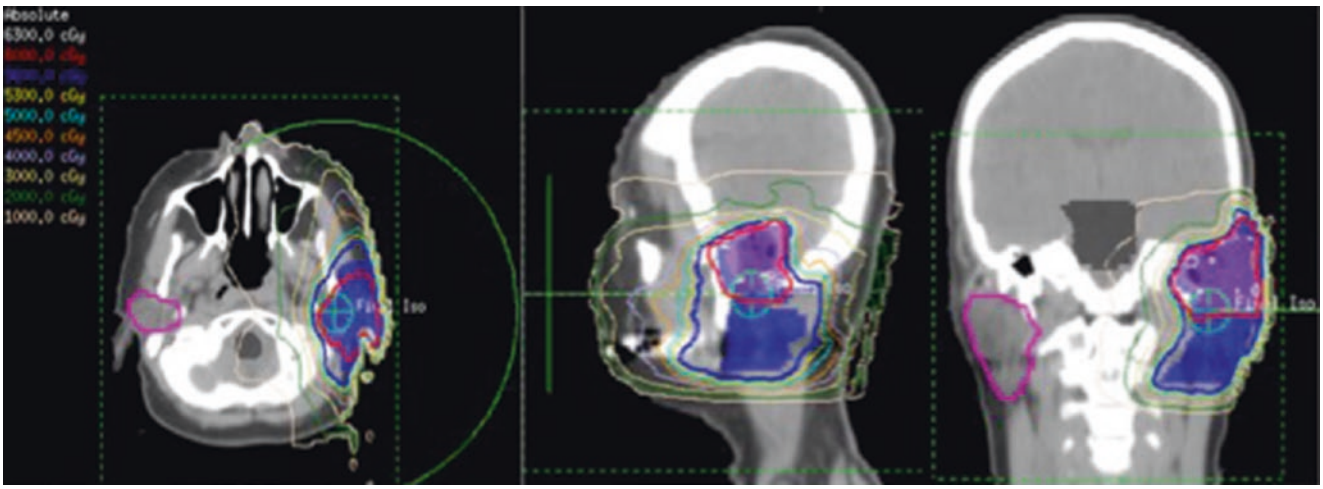


**Fig. 29.20** Final dose distribution plan. Red, tumor bed, 60 Gy; blue, non-involved surgical bed, 56 Gy. Note excellent dose sparing of contralateral parotid gland and minimal dose to the left temporal lobe

Common local side effects for radiotherapy to the temporal bone region include radiation dermatitis, reduced hearing due to swelling of the ear canal, and thickened saliva and/or xerostomia. Oral mucositis and altered sense of taste can be common if the oral cavity, particularly the oral tongue, receives more than 30 Gy. Esophagitis is less common in this group of patients as they tend to receive unilateral neck treatment, reducing the dose to the esophagus compared to other head and neck cancer patients with bilateral neck irradiation.

These side effects typically increase in severity over the treatment course and resolve in approximately 4–6 weeks after completion of treatment. Fatigue and dysgeusia may take several months to resolve.

## Radiation-Associated Long-Term Effects on the Temporal Bone

For long-term head and neck cancer survivors who received radiotherapy to the temporal bone, vigilant surveillance of late complications to the temporal bone is of upmost importance to allow optimal management.

Radiation therapy can cause tissue fibrosis, in particular vascular fibrosis and intimal hyperplasia leading to decreased vascular supply to the irradiated normal tissue. Within the temporal bone region, this contributes to the risk of long-term injury to bone (osteonecrosis), cartilage (chondronecrosis), cochlea (sensorineural hearing loss), and Eustachian tube/middle ear (serous otitis media and/or conductive hearing loss). Although the risk of developing these long-term effects is dependent on the total radiation dose and dose/fraction received, the patient's age, smoking status, comorbidities, and previous surgery to the area are also contributing factors.

Typically, sensorineural hearing loss and otitis media tend to develop within months after radiation treatment due to the fibrosis of the cochlea and Eustachian tube. A total cochlear dose of 30–50 Gy is an independent risk factor for sensorineural hearing loss, while the dose-effect relationship for the Eustachian tube is less well-established and is estimated at approximately 43–50 Gy [13].

Osteonecrosis of the temporal bone can develop 5–10 years after radiotherapy. Patients usually have non-specific symptoms such as crusting of external auditory canal, otorrhea, otalgia, and/or hearing loss. Physicians need to have high index of suspicion to identify and diagnose these patients as early osteonecrosis can be managed conservatively or with hyperbaric oxygen, whereas advanced or symptomatic osteonecrosis, in most cases, will require surgical intervention. It is estimated that a dose of 50Gy and above is a risk factor [13].

Radiation therapy can cause vascular changes including microangiopathy in the brain [14]. The temporal lobe is at risk, although low, of developing radiation necrosis given its location adjacent to the temporal bone. Encephalomalacia of the temporal lobe is usually asymptomatic but can manifest with non-specific symptoms such as headaches, mood changes, gradual memory impairment, fatigue, and poor concentration. Given the rarity of radiation necrosis of the brain, the majority of cases of temporal lobe necrosis tend to be reported in patients who received definitive radiotherapy for nasopharyngeal carcinoma. The median time to develop temporal lobe necrosis is typically 5 years [15]. A large imaging study on 1916 patients who received definitive radiotherapy for nasopharyngeal carcinoma over a 5-year period showed only 47 (2.5%) patients demonstrated temporal lobe changes on imaging [15].

## Conclusion

Overall, radiation therapy improves locoregional control in patients with temporal bone tumors. For unresectable locally advanced tumors, radiotherapy can be utilized upfront as a definitive treatment. Regardless, in all cases, careful radiation treatment planning is necessary due to the presence of critical radiosensitive normal structures within the region. Various methods of treatment delivery and radiation modalities can be used to achieve the optimal radiotherapy plan for the patient.

## References


1. Zanoletti E, Lovato A, Stritoni P, Martini A, Mazzoni A, Marioni G. A critical look at persistent problems in the diagnosis, staging and treatment of temporal bone carcinoma. Cancer Treat Rev. 2015;41(10):821–6. https://doi.org/10.1016/j.ctrv.2015.10.007.
2. Masterson L, Rouhani M, Donnelly NP, Tysome JR, Patel P, Jefferies SJ, et al. Squamous cell carcinoma of the temporal bone: clinical outcomes from radical surgery and postoperative radiotherapy. Otol Neurotol. 2014;35(3):501–8. https://doi.org/10.1097/MAO.0000000000000265.
3. Moffat DA, Wagstaff SA, Hardy DG. The outcome of radical surgery and postoperative radiotherapy for squamous carcinoma of the temporal bone. Laryngoscope. 2005;115(2):341–7. https://doi.org/10.1097/01.mlg.0000154744.71184.c7.
4. Zhang T, Li W, Dai C, Chi F, Wang S, Wang Z. Evidence-based surgical management of T1 or T2 temporal bone malignancies. Laryngoscope. 2013;123(1):244–8. https://doi.org/10.1002/lary.23637.
5. Cristalli G, Mercante G, Marucci L, Soriani A, Telera S, Spriano G. Intraoperative radiation therapy as adjuvant treatment in locally advanced stage tumours involving the middle ear: a hypothesis-generating retrospective study. Acta Otorhinolaryngol Ital. 2016;36(2):85–90. https://doi.org/10.14639/0392-100X-486.
6. Pfreundner L, Schwager K, Willner J, Baier K, Bratengeier K, Brunner FX, et al. Carcinoma of the external auditory canal and middle ear. Int J Radiat Oncol Biol Phys. 1999;44(4):777–88.
7. Bibas AG, Ward V, Gleeson MJ. Squamous cell carcinoma of the temporal bone. J Laryngol Otol. 2008;122(11):1156–61. https://doi.org/10.1017/S0022215107001338.
8. Prasad SC, D'Orazio F, Medina M, Bacciu A, Sanna M. State of the art in temporal bone malignancies. Curr Opin Otolaryngol Head Neck Surg. 2014;22(2):154–65. https://doi.org/10.1097/MOO.0000000000000035.
9. Ogawa K, Nakamura K, Hatano K, Uno T, Fuwa N, Itami J, et al. Treatment and prognosis of squamous cell carcinoma of the external auditory canal and middle ear: a multi-institutional retrospective review of 87 patients. Int J Radiat Oncol Biol Phys. 2007;68(5):1326–34. https://doi.org/10.1016/j.ijrobp.2007.01.052.
10. Morita S, Homma A, Nakamaru Y, Sakashita T, Hatakeyama H, Kano S, et al. The outcomes of surgery and chemoradiotherapy for temporal bone cancer. Otol Neurotol. 2016;37(8):1174–82. https://doi.org/10.1097/MAO.0000000000001152.
11. Shinomiya H, Hasegawa S, Yamashita D, Ejima Y, Kenji Y, Otsuki N, et al. Concomitant chemoradiotherapy for advanced squamous cell carcinoma of the temporal bone. Head Neck. 2016;38(Suppl 1):E949–53. https://doi.org/10.1002/hed.24133.
12. Takenaka Y, Cho H, Nakahara S, Yamamoto Y, Yasui T, Inohara H. Chemoradiation therapy for squamous cell carcinoma of the external auditory canal: a meta-analysis. Head Neck. 2015;37(7):1073–80. https://doi.org/10.1002/hed.23698.
13. Lambert EM, Gunn GB, Gidley PW. Effects of radiation on the temporal bone in patients with head and neck cancer. Head Neck. 2016;38(9):1428–35. https://doi.org/10.1002/hed.24267.
14. Valk PE, Dillon WP. Radiation injury of the brain. AJNR Am J Neuroradiol. 1991;12(1):45–62.
15. Chong VF, Fan YF, Mukherji SK. Radiation-induced temporal lobe changes: CT and MR imaging characteristics. AJR Am J Roentgenol. 2000;175(2):431–6. https://doi.org/10.2214/ajr.175.2.1750431.